Transmittance signal in real ladder-type atoms

Heung-Ryoul Noh[1,*] and Han Seb Moon[2,†]
[1]*Department of Physics, Chonnam National University, Gwangju KR-500-757, Korea*
[2]*Department of Physics, Pusan National University, Busan KR-609-735, Korea*
(Received 24 November 2011; published 19 March 2012)

We clarify an interpretation of transmittance signals in ladder-type atomic systems by discriminating the contributions of one-photon resonance, two-photon resonance, and a mixed term of both in the calculated spectra for these ladder-type multilevel atoms. When the two-photon-resonance effect is distinguished from an accurate spectrum calculated by modeling ladder-type electromagnetically-induced transparency for the $5S_{1/2} - 5P_{3/2} - 5D_{5/2}$ transitions of ^{87}Rb atoms, we find that the transmittance signals for the $5D_{5/2}(F'' = 2,3)$ states are mainly composed of the mixed term related not to pure-two-photon atomic coherence but to the optical-pumping effect whereas the transmittance signal for the $5D_{5/2}(F'' = 4)$ state originates from both the pure-two-photon-resonance term and the mixed term.

DOI: 10.1103/PhysRevA.85.033817 PACS number(s): 42.50.Gy, 32.80.Qk, 32.80.Wr

I. INTRODUCTION

Coherent interaction of several laser lights via an atomic medium has induced the flourishing development of nonlinear laser spectroscopy such as coherent-population trapping (CPT) [1] and electromagnetically-induced transparency (EIT) [2] and absorption (EIA) [3]. These subjects are being intensively investigated due to their possible applications in fields such as atomic clocks [4], quantum information [5], light storage [6], and precision magnetometers [7]. EIT can be observed in various atomic systems such as Λ, V, and ladder (or cascade) schemes [2]. Among these, the Λ scheme has attracted considerable interest because of the very narrow linewidth that can be obtained compared to those of other schemes. Recently, however, the ladder scheme has also drawn much attention as it can be used in the study of Rydberg states [8], multiwave mixing [9], the coherent control of polarization [10], atomic filters [11], and laser spectroscopy via excited states [12].

Ladder-type EIT has been demonstrated in many kinds of atoms, including sodium [13], rubidium [14–19], and cesium [20]. In the case of ladder-type atomic systems in alkali-metal atoms, the two-photon atomic coherence and the optical-pumping effects cannot be distinguished from changes in the EIT spectrum; this is because the frequency of double-resonance optical pumping (DROP) occurs under the conditions of two-photon resonance in a similar manner to that of EIT [21]. A further, serious problem is that the transmittance signal due to optical pumping is often confused with EIT in many studies of ladder-type EIT in alkali-metal atoms [13–20]. The basis of this misunderstanding is that in EIT real ladder-type atoms are modeled as simple three-level atomic systems without including the DROP effect [19].

A rigorous analytical theory for three-level atoms was reported in 1995 [15]. However, many papers' theoretical work is simply based on a simplified three-level model, and more detailed studies which consider realistic atomic-energy levels, to the best of our knowledge, do not exist. For the interesting topic of discrimination of one-photon and two-photon resonances in the EIT signals, there have been theoretical studies on three-level atoms [22–24] and experimental works on Na [13] and Rb [21]. It should be noted that the quantum-jump approach has been used for the probe response in the three-level atomic systems [25,26]. However, no detailed calculations that discriminate between these two effects in real atoms have been reported. In addition, although atomic coherence and optical pumping significantly affect the polarization of the lasers interacting with the atoms, due to the different transition probabilities related to the laser polarization and hyperfine states [27], the simple three-level atomic model cannot account for the polarization dependence of the signals in real ladder-type atoms.

Since the potential applications of EIT mainly make use of its very narrow absorption (or very steep dispersion) signals, which is attributed to two-photon atomic coherence, it is a very important and fundamental problem in laser spectroscopy to accurately calculate and discriminate the effects of two-photon coherence and two-photon resonance. In this paper we present a general method for calculating an accurate spectrum and discriminating the contribution of the two-photon resonance effect in this spectrum for real ^{87}Rb atoms using ladder-type EIT. In addition to this specific scheme, our proposed method can be generally applied to laser spectroscopy, including almost all cases of EIT and EIA in which laser lights with two colors are involved. In particular, this method can be used to accurately calculate and discriminate the contribution of the two-photon-resonance effect in EIT for Rydberg atoms [19]. In this paper, we study three aspects of ladder-type EIT for ^{87}Rb atoms: accurate calculation of the EIT spectrum, discrimination of the one-photon- and two-photon-resonance effects in the signal, and polarization dependence.

II. THEORY

We calculated the EIT spectrum for the $5S_{1/2} - 5P_{3/2} - 5D_{5/2}$ transitions of ^{87}Rb atoms. Figure 1 shows a diagram of the energy levels under consideration. A probe laser of wavelength $\lambda_1 = 780$ nm scans around the transition line $5S_{1/2} - 5P_{3/2}$ while a coupling laser of wavelength $\lambda_2 = 775.8$ nm is locked on the transition $5P_{3/2} - 5D_{5/2}$. We calculated the density-matrix equation, including all the relevant

*hrnoh@chonnam.ac.kr
†hsmoon@pusan.ac.kr

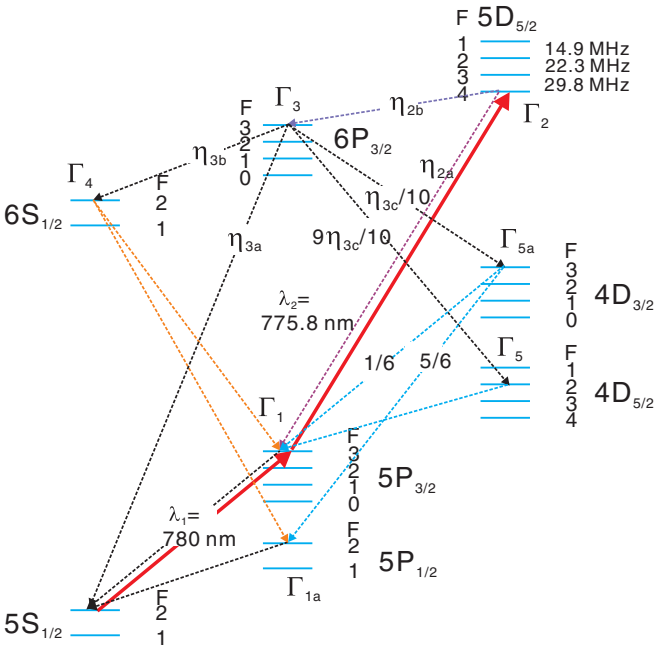

FIG. 1. (Color online) Energy-level diagram for the transitions $5S_{1/2} - 5P_{3/2} - 5D_{5/2}$ of ^{87}Rb atoms. The decay rates of the states $5P_{3/2}$, $5P_{1/2}$, $5D_{5/2}$, $6P_{3/2}$, $6S_{1/2}$, $4D_{5/2}$, and $4D_{3/2}$ are given by $\Gamma_1(=2\pi 6.065$ MHz) [28], $\Gamma_{1a}(=2\pi 5.746$ MHz) [28], $\Gamma_2(=2\pi 0.6673$ MHz) [29], $\Gamma_3(=2\pi 1.3$ MHz) [30], $\Gamma_4(=2\pi$ 3.492 MHz) [31], $\Gamma_5(=2\pi 1.7$ MHz) [32], and $\Gamma_{5a}(=2\pi 1.8$ MHz) [32], respectively. The branching ratios are $\eta_{2a} = 0.74$, $\eta_{2b} = 0.26$, $\eta_{3a} = 0.23$, $\eta_{3b} = 0.55$, and $\eta_{3c} = 0.22$ [32].

magnetic sublevels for the states $5S_{1/2}(F = 2)$, $5P_{3/2}(F' = 3)$, and $5D_{5/2}(F'' = 2,3,4)$. As can be seen in Fig. 1, there exist other states that are not directly coupled to the laser beams. Including the remaining sublevels in the states $5S_{1/2}(F = 2)$, $5P_{3/2}(F' = 3)$, and $5D_{5/2}(F'' = 2,3,4)$, we also describe all relaxation and optical-pumping phenomena using the rate equations for all other states.

We assume that the probe and coupling lasers are aligned colinearly and are counterpropagating. We consider six polarization configurations of the coupling-probe lasers: (i) $\pi \parallel \pi$, (ii) $\pi \perp \pi$, (iii) $\pi - \sigma^+$, (iv) $\sigma^+ - \sigma^+$, (v) $\sigma^+ - \sigma^-$, and (vi) $\sigma^+ - \pi$. The incident electric fields of the probe and the coupling beams with a given coordinate system are described by $\vec{E}_p = E_{0p}[c_+\hat{\epsilon}_+ + c_0\hat{\epsilon}_0 + c_-\hat{\epsilon}_-]e^{-i\omega_1 t}$ and $\vec{E}_c = E_{0c}[a_+\hat{\epsilon}_+ + a_0\hat{\epsilon}_0 + a_-\hat{\epsilon}_-]e^{-i\omega_2 t}$, respectively, where E_{0p} (E_{0c}) is the magnitude of the electric field of the probe (coupling) beam and $\omega_{1(2)} = 2\pi c/\lambda_{1(2)}$. The coefficients for the π- [σ^+]-polarized coupling beam are $(a_+,a_0,a_-) = (0,1,0)$ [(1,0,0)]. The coefficients (c_+,c_0,c_-) for the probe beam are (i) (0,1,0), (ii) $(-1/\sqrt{2},0,1/\sqrt{2})$, (iii) $(i/2,-1/\sqrt{2},-i/2)$, (iv) (1,0,0), (v) (0,0,1), and (vi) $(-1/\sqrt{2},0,1/\sqrt{2})$. The susceptibility of each component of the electric field is then given by [33]

$$\chi_q = -N_{\rm at}\frac{3\lambda_1^3}{4\pi^2}\frac{\Gamma_1}{\Omega_1}\frac{1}{c_q}\sum_{m=-2}^{2} C_{F=2,m}^{F'=3,m+q}\sigma_{F=2,m}^{F'=3,m+q}, \qquad (1)$$

where $C_{F,m}^{F',m'}$ and $\sigma_{F,m}^{F',m'}$ are the normalized transition-coefficient and density-matrix elements between the states $|F,m\rangle$ and $|F',m'\rangle$, respectively [34]. Ω_1 is the Rabi frequency of the probe beam.

After traversing an infinitesimal distance of dz, the intensity of the probe beam is changed by $-I_0\alpha dz$, where I_0 is the intensity of the incidence probe beam. Therefore, the absorption coefficient is given by $\alpha_0 = \mathrm{Im}\sum_{q=-1}^{1}[k_1|c_q|^2\chi_q]$, where $k_1 = 2\pi/\lambda_1$. Finally, the absorption coefficient averaged over the velocity distribution and transit times is given by

$$\alpha(\delta_p) = \frac{1}{t_{\rm av}}\int_0^{t_{\rm av}} dt\int_0^{\infty} dv\,\frac{1}{\sqrt{\pi}u}e^{-(v/u)^2}\alpha_0(v,t),$$
$$\alpha_0 = -N_{\rm at}\frac{3\lambda_1^2}{2\pi}\frac{\Gamma_1}{\Omega_1}\mathrm{Im}\left[\sum_{q=-1}^{1}\sum_{m=-2}^{2} c_q^* C_{F=2,m}^{F'=3,m+q}\sigma_{F=2,m}^{F'=3,m+q}\right], \qquad (2)$$

where u is the most probable speed of the atom, $N_{\rm at}$ is the atomic density, the average transit time is given by $t_{\rm av} = (\sqrt{\pi}/2)d/u$, and d is the diameter of the laser beam [34]. We refer the reader to Ref. [34] for the detailed method of calculating the density-matrix elements at given t and v. When the number of the nonvanishing coefficients of the probe beam is greater than one, multiple Zeeman and optical coherences between the sublevels in $5P_{3/2}(F' = 3)$ and in $5S_{1/2}(F = 2)$ exist via multiphoton interactions. In the calculation, we consider these interactions up to the two-photon level; this is realistic because the intensity of the probe beam is a lot weaker than the saturation intensity.

As described in previous reports for three-level atoms [23,24], the coherences between the intermediate and ground states can be decomposed into two parts: (i) the population difference term, which is composed of the populations in the intermediate and ground states, and (ii) the coherence term, which is composed of the coherences between the excited and ground states. Extending this analysis to the multilevel atoms, the absorption coefficient is given by $\alpha = \alpha_{\rm pop} + \alpha_{\rm coh}$, where $\alpha_{\rm pop}$ and $\alpha_{\rm coh}$ represent the population-difference contribution and coherence contribution, respectively. For example, when the polarization configuration is $\pi \parallel \pi$, $\alpha_{\rm pop}$ and $\alpha_{\rm coh}$ are given by

$$\alpha_{\rm pop} = -N_{\rm at}\frac{3\lambda_1^2}{2\pi}\frac{\Gamma_1}{\Omega_1}\frac{\Gamma_1\Omega_1}{4\delta_1^2+\Gamma_1^2}\big[(1/3)\big(Q_3^{-2}-P_2^{-2}\big) + (8/15)\big(Q_3^{-1}-P_2^{-1}\big) + (3/5)\big(Q_3^{0}-P_2^{0}\big) + (8/15)\big(Q_3^{1}-P_2^{1}\big) + (1/3)\big(Q_3^{2}-P_2^{2}\big)\big],$$
$$\alpha_{\rm coh} = \alpha - \alpha_{\rm pop}, \qquad (3)$$

respectively, where $\delta_1 = \delta_p - k_1 v$ and P_2^m and Q_3^m represent the populations of the states $|F = 2,m\rangle$ and $|F' = 3,m\rangle$, respectively. Equation (3) is also averaged by an analogous method seen in Eq. (2). We can obtain similar expressions for the other polarization configurations in the same way as Eq. (3).

Extending the diagrammatical analysis for the three-level atom seen in Ref. [24] to real multilevel atoms, we describe how to discriminate the three contributions in the EIT spectrum for ^{87}Rb atoms: the pure-one-photon-resonance contribution, the pure-two-photon-resonance contribution, and the mixed term from both resonances.

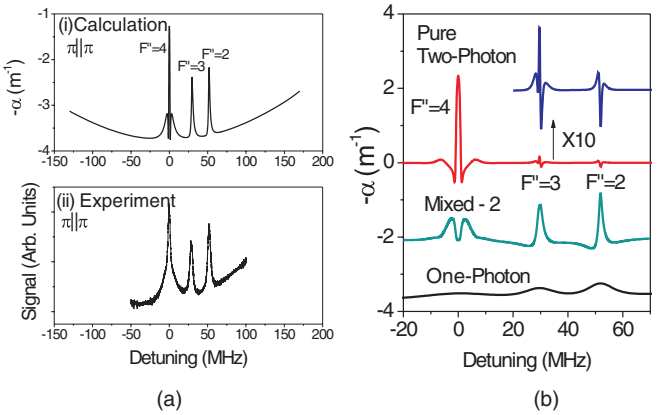

FIG. 2. (Color online) (a) The EIT spectra for the $\pi \parallel \pi$-polarization configuration for the (i) calculated and (ii) experimental results. (b) The calculated results for the pure-two-photon, mixed, and one-photon contributions.

A. The pure-one-photon-resonance effect (α_{1p})

This contribution can be obtained from α by ignoring the optical coherences between the ground and the excited states. When the density-matrix equations are established, we set the optical coherences between the ground state ($5P_{1/2}$) and the excited state ($5D_{5/2}$) to zero. Then, we can obtain the pure-one-photon-resonance term (α_{1p}) as follows:

$$\alpha_{1p} = \alpha \quad \text{with} \quad \sigma_{F=2,m}^{F''=3,m''} = 0.$$

Note that in this case, α_{coh} vanishes. Unlike the simple three-level atom, there exist many matrix elements for real atoms. It should be noted that the matrix elements are strongly dependent on the choice of polarization configuration.

B. The pure-two-photon-resonance effect (α_{2p})

As described in Ref. [24], the pure-two-photon-resonance effect can be calculated from the coherence term (α_{coh}) in Eq. (3) by setting the population in each magnetic sublevel of the ground state to $1/8$ whereas the populations in the intermediate and excited states are 0. In sum, we have

$$\alpha_{2p} = \alpha_{\text{coh}} \quad \text{with} \quad P_2^m = 1/8 \text{ and other populations} = 0.$$

We note that the Zeeman coherences in the ground or the intermediate states must vanish.

C. The mixed term (α_{mix})

This contribution is given by subtracting the pure-one-photon-resonance term and the pure-two-photon-resonance term from the total absorption coefficient (α) as follows:

$$\alpha_{\text{mix}} = \alpha - \alpha_{1p} - \alpha_{2p}.$$

III. RESULTS

The results for the $\pi \parallel \pi$-polarization configuration are shown in Fig. 2. In Fig. 2(a), the upper trace shows the calculated total signal, and the lower trace presents the experimental result reported in Ref. [27]. In the experimental results, the intensities of the probe and the coupling beams are 15 μW and 8.2 mW, respectively. The diameters of the lasers are 2.0 mm. Figure 2(b) shows the decomposition of the calculated signal; the pure-two-photon, the mixed, and the one-photon contributions are presented. From Fig. 2(a), we can see there is a good agreement between the calculated and experimental results. It should be noted that the sharp dip in the signal seen in the calculated results, originating from the wavelength mismatch between the probe and the coupling lasers [18], is not seen in the experimental results. This results from the relatively large linewidths of the probe and coupling lasers, which are respectively $\sim$1 MHz. In Fig. 2(b), we can see that pure-two-photon signals for $F'' = 2$ and $F'' = 3$ are very weak. As such, we can conclude the signals for $F'' = 2$ and $F'' = 3$ mainly come from α_{1p} and α_{mix}. This is because of the weak relative strengths between the states $5P_{3/2}(F' = 3)$ and $5D_{5/2}(F'' = 2,3)$. In contrast, the pure-two-photon signal for $F'' = 4$ is very strong. Although the transitions between the states $5P_{3/2}(F' = 3)$ and $5D_{5/2}(F'' = 4)$ are not completely cycling and because the transition strength is strong and the branching ratio ($\eta_{2a} = 0.74$) is quite large, the signal is composed of all three contributions simultaneously. We can

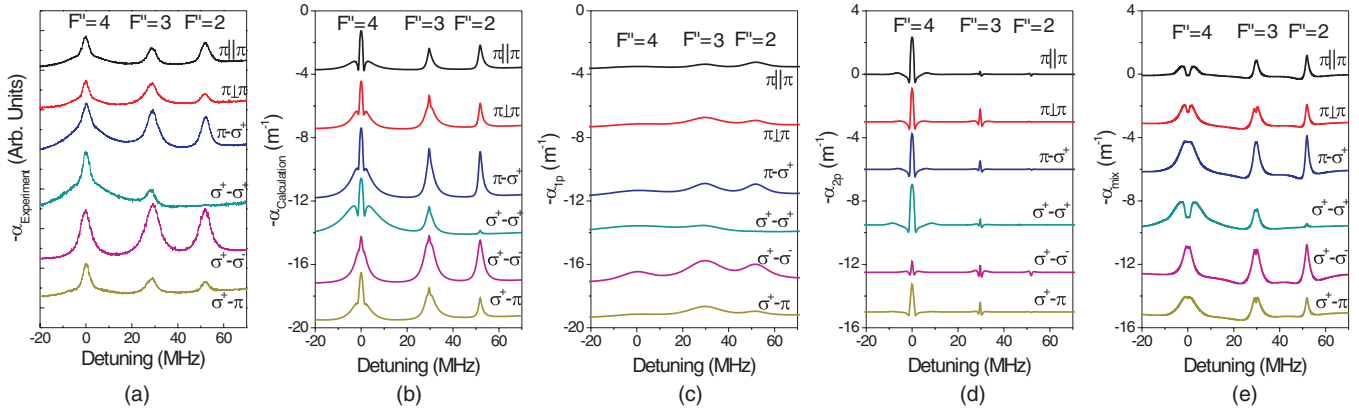

FIG. 3. (Color online) The results for six polarization configurations: (a) the experimental results; (b) calculated results; and (c) one-photon contributions, (d) pure-two-photon contributions, and (e) mixed contributions of the calculated results. Absolute values of the absorption coefficients are correct only for $\pi \parallel \pi$ while the scales for other configurations are displaced for clear display.

see that a narrow signal results from the pure-two-photon contribution while the broad signal results are mainly due to the mixed term.

The results for each of the six polarization configurations are shown in Fig. 3. The experimental and calculated results are presented in Figs. 3(a) and 3(b), respectively. The one-photon, pure-two-photon, and mixed contributions of the calculated results are shown in Figs. 3(c), 3(d), and 3(e), respectively. In each figure, we show the results for the polarization configurations $\pi \parallel \pi, \pi \perp \pi, \pi - \sigma^+, \sigma^+ - \sigma^+$, $\sigma^+ - \sigma^-$, and $\sigma^+ - \pi$ in that order from the top of the figure. Comparing the spectra shown in Figs. 3(a) and 3(b), we see that the calculated results are in good agreement with the experimental results. Note that the sharp two-photon-resonance signals become broadened due to the finite linewidth of the lasers. It is interesting that the signal for $F'' = 2$, when the polarization configuration is $\sigma^+ - \sigma^+$, is almost invisible. This is because when $m \leqslant 2$, the populations at the states $5S_{1/2}(F = 2, m - 1)$ and $5P_{3/2}(F' = 3, m)$ become very small due to optical pumping. In addition, all states except for $5S_{1/2}(F = 2, m = 2)$ are not coupled to the excited state in this polarization configuration. Therefore, the signal for the transitions $5S_{1/2}(F = 2) - 5P_{3/2}(F' = 3) - 5D_{5/2}(F'' = 2)$ becomes very weak.

From the decomposition of the calculated results presented in Figs. 3(c), 3(d), and 3(e), we find that the narrow and broad signals result mainly from the pure-two-photon and mixed contributions, respectively. As can be seen in Fig. 2, the pure-two-photon signals for $F'' = 2, 3$ are very weak, but the signal for $F'' = 4$ is strong. When the polarization configuration is $\sigma^+ - \sigma^-$, however, we can see that the pure-two-photon-resonance signal for $F'' = 4$ is very weak. This can be attributed to the effective two-photon-transition strengths. The ratios of the transition strengths for the configurations $\sigma^+ - \sigma^-$, $\sigma^+ - \sigma^+$, and $\pi \parallel \pi$ are approximately 1, 6, and 4, respectively. Due to this weak effective transition strength, the two-photon-resonance contribution is very small for the $\sigma^+ - \sigma^-$-polarization configuration.

IV. CONCLUSIONS

In summary, we presented a theoretical study on the accurate calculation of line shapes in EIT for the $5S_{1/2} - 5P_{3/2} - 5D_{5/2}$ transitions of ^{87}Rb atoms. All possible transitions were considered in the calculation. As the time-dependent density-matrix equations were solved numerically, no phenomenological constant was used. In addition, we were able to discriminate the effects of one-photon and two-photon resonances in the EIT spectra. In the case of signals with weaker transition strengths, such as those from the states of $|F'' = 2\rangle$ or $|F'' = 3\rangle$, the signals are mainly composed of the mixed term. In contrast, the signals from the states with strong transition strengths are composed of both the pure-two-photon-resonance term and the mixed term although these transitions are not completely cycling. From the calculations for different polarization configurations, we can account for the observed experimental results. The method of calculation described in this paper is applicable generally to other systems with different energy levels or other atomic species and could even be used with Λ or V schemes. Experimental and theoretical work on other transition lines of ^{87}Rb and ^{85}Rb atoms is currently in progress.

ACKNOWLEDGMENTS

This research was supported by the Basic Science Research Program through the National Research Foundation of Korea funded by the Ministry of Education, Science and Technology (Grants No. 2011-0009886 and No. 2009-0073051).

[1] E. Arimondo, Prog. Opt. **35**, 257 (1996).
[2] M. Fleischhauer, A. Imamoglu, and J. P. Marangos, Rev. Mod. Phys. **77**, 633 (2005).
[3] A. M. Akulshin, S. Barreiro, and A. Lezama, Phys. Rev. A **57**, 2996 (1998).
[4] J. Vanier, Appl. Phys. B **81**, 421 (2005).
[5] K. Hammerer, A. S. Sørensen, and E. S. Polzik, Rev. Mod. Phys. **82**, 1041 (2010).
[6] M. D. Lukin, Rev. Mod. Phys. **75**, 457 (2003).
[7] D. Budker and M. V. Romalis, Nat. Phys. **3**, 227 (2007).
[8] M. Saffman, T. G. Walker, and K. Mølmer, Rev. Mod. Phys. **82**, 2313 (2010).
[9] Y. Zhang, U. Khadka, B. Anderson, and M. Xiao, Phys. Rev. Lett. **102**, 013601 (2009).
[10] R. Drampyan, S. Pustelny, and W. Gawlik, Phys. Rev. A **80**, 033815 (2009).
[11] S. Liu, Y. Zhang, H. Wu, and P. Yuan, J. Opt. Soc. Am. B **28**, 1100 (2011).
[12] C. Carr, C. S. Adams, and K. J. Weatherill, Opt. Lett. **37**, 118 (2012).
[13] N. Hayashi, A. Fujisawa, H. Kido, K. Takahashi, and M. Mitsunaga, J. Opt. Soc. Am. B **27**, 1645 (2010).
[14] R. R. Moseley, S. Shepherd, D. J. Fulton, B. D. Sinclair, and M. H. Dunn, Opt. Commun. **119**, 61 (1995).
[15] J. Gea-Banacloche, Y. Q. Li, S. Z. Jin, and M. Xiao, Phys. Rev. A **51**, 576 (1995).
[16] S. Wielandy and A. L. Gaeta, Phys. Rev. A **58**, 2500 (1998).
[17] S. D. Badger, I. G. Hughes, and C. S. Adams, J. Phys. B **34**, L749 (2001).
[18] A. Krishna, K. Pandey, A. Wasan, and V. Natarajan, Europhys. Lett. **72**, 221 (2005).
[19] A. K. Mohapatra, T. R. Jackson, and C. S. Adams, Phys. Rev. Lett. **98**, 113003 (2007).
[20] J. J. Clarke, W. A. van Wijngaarden, and H. Chen, Phys. Rev. A **64**, 023818 (2001).
[21] H. S. Moon and H. R. Noh, J. Phys. B **44**, 055004 (2011).
[22] T. Y. Abi-Salloum, J. Mod. Opt. **57**, 1366 (2010).
[23] H. R. Noh and H. S. Moon, Opt. Express **19**, 11128 (2011).
[24] H. R. Noh and H. S. Moon, Phys. Rev. A **84**, 053827 (2011).
[25] J. Mompart and R. Corbalán, Phys. Rev. A **63**, 063810 (2001).

[26] J. Mompart and R. Corbalán, J. Opt. Soc. Am. B **20**, 2386 (2003).
[27] H. S. Moon and H. R. Noh, Phys. Rev. A **84**, 033821 (2011).
[28] P. Siddons, C. S. Adams, C. Ge, and I. G. Hughes, J. Phys. B **41**, 155004 (2008).
[29] D. Sheng, A. Perez Galvan, and L. A. Orozco, Phys. Rev. A **78**, 062506 (2008).
[30] S. Vdović, T. Ban, D. Aumiler, and G. Pichler, Opt. Commun. **272**, 407 (2007).
[31] E. Gomez, F. Baumer, A. D. Lange, G. D. Sprouse, and L. A. Orozco, Phys. Rev. A **72**, 012502 (2005).
[32] M. S. Safronova, C. J. Williams, and C. W. Clark, Phys. Rev. A **69**, 022509 (2004).
[33] D. Meschede, *Optics, Light and Lasers* (Wiley-VCH, Weinheim, 2007).
[34] H. R. Noh and H. S. Moon, Phys. Rev. A **80**, 022509 (2009).